Multivariable Control of Multi-Zone Chemical Mechanical Polishing

Sheng-Jyh Shiu[1], Cheng-Ching Yu[*1], Shih-Haur Shen[2], and An-Jhih Su [1]

[1]Dept. of Chem. Eng., National Taiwan UniversitTaipei 106-17, TAIWAN
[2]Applied Materials Taiwan Ltd., Hsin-Chu 300, TAIWAN

Abstract: The modeling and multivariable control of the multi-zone chemical mechanical polishing (CMP) is studied in this work. For a three-zone CMP, the copper thickness across the radial position is measured with an in-situ sensor and then the measurements are converted to 60 data points across the radial position. In the process control notation, these are the controlled variables and the manipulated variables are the three pressures applied to each zone. Therefore, this is a 60x3 non-square multivariable control problem. Thus, a 60x3 steady-state gain matrix is obtained followed by finding dynamic elements according to the gas holdup in each chamber. As a result of the non-square system, it is not possible to keep all 60 outputs at their set points using only 3 inputs. The singular value decomposition (SVD) is used to design a non-square feedback controller. The proposed control system is test on incoming wafers with different surface profiles. Results show that achievable performance can be maintained using the proposed SVD controller. *Copyright © 2004 IFAC*

Keywords: CMP, multi-zone CMP, multivariable control, non-square system.

1. INTRODUCTION

In Cu CMP, the copper is removed using a two-step procedure. First, the overburden Cu is removed with a high removal rate and the objective is to reduce the step height to a given specification with a certain amount of copper remains. The reason for stopping short from the oxide surface is that within-wafer non-uniformity (WIWNU), as the results of incoming profile and CMP process, is often encountered in Cu CMP and the remaining Cu layer prevents unnecessary dishing in the thin spots on the wafer. This is followed by the overpolishing step where overburden metal and some barrier are removed and this step is generally carried out using a much smaller removal rate [Kao et al., 2002, Edgar et al., 2000, and Yao et al., 2000]. As implied by the name, CMP removes overburden metal or unnecessary materials by the combinative effects of mechanical abrasion and chemical reactions.

Despite recent advances in CMP, some manufacturing concerns associated with successful implementation of CMP remain to be overcome. In theory, CMP can achieve global planarity, but there is still a problem that different operating conditions will result in non-uniformity in thickness of wafer surface. The WIWNU indicates the variation in surface thickness across the wafer radial position, especially on the edge. Besides, the surface profile of wafers produced from electrochemical plating (ECP) process appears that the metallic layer is thicker on edge area. Thus, a new type of CMP, multi-zone CMP, offers an attractive alternative. Multi-zone CMP is expected to reduce WIWNU and to provide a wider processing window. Unlike the typical single zone configuration, the wafer carrier is divided into multiple zones in the radial position and different pressure can be applied to each zone (Fig. 1). The objective of this work is to devise a systematic approach to the modeling and control of such CMP processes.

corresponding author; e-mail: ccyu@ntu.edu.tw; fax: +886-2-2362-3040

2. MULTI-ZONE CMP

2.1. Process Description.

Consider a CMP system where the wafer carrier is divided into three zones in the radial position and different pressure can be applied to each zone (Fig. 1). For a wafer carrier with the radius of 150mm (i.e., a 300 mm wafer), zone #1 covers 0-130mm, the second zone ranges from 130-140mm, and third zone covers 140mm and beyond. Typically, the well-known Preston's equation [Preston, 1927] is used to model the polishing process. It describes the material removal as a linear function of pressure and rotation speed.

$$RR = K_p \cdot p \cdot v \qquad (1)$$

where K_p is the Preston constant, p is pressure, and v is rotation speed. The Preston equation can be extended to multi-zone CMP in a straightforward manner. For the multi-zone system, the relationship between removal rate at the ith radial position and input variables can be expressed as:

$$RR_i = \sum_j K_{p,i,j}\, p_j \cdot v \qquad (2)$$

where $K_{p,i,j}$ is the local Preston constant describing the effect of pressure from jth zone on the ith radial position, pj denotes the pressure of the jth zone, and v is again the rotation speed. Without loss of generality, assume that the rotation speed is fixed throughout all runs and v is absorbed into $K_{p,i,j}$ for the subsequent development.

2.2. Design of Experiments (DOE)

Copper (Cu) CMP is carried out on an Applied Materials' Reflexion™ polisher using Titan Profiler™ polishing heads. Polishing pad (Rodel IC1010) is used and the experimental copper CMP slurry is provided by Cabot Corporation. Electrochemical plating (ECP) process is employed for Cu plating. The 300mm wafers without pattern are used in all tests. All copper thickness measurements are performed with an *in situ* i-Scan sensor.

All the experiments were carried out according to a standard design of experiment procedure (DOE). The factors in this work are the three pressures applied to each zone and a pressure applied to the retaining ring (i.e., keeping the wafer in proper position). From center of the wafer to the edge, they are defined as p_1, p_2, p_3, and p_{rr}, respectively. We devise two levels for each factor such that a four-factor and two-level design of experiment (DOE) is carried out.

Before the test proceeds, the surfaces of 20 blanket wafers are measured. There are 119 measurement points from one edge to the other, so the pre-CMP thickness is defined as:

$$\mathbf{z_0} = \left[z_{0,1}, z_{0,2}, \ldots, z_{0,119} \right]^T \qquad (3)$$

The subscript 0 denotes the initial condition and i represents the radial position across the wafer. The post-CMP thickness is also recorded after polishing for 60 seconds.

$$\mathbf{z} = \left[z_1, z_2, \ldots, z_{119} \right]^T \qquad (4)$$

Because of the symmetry of wafers and the applied pressures, an averaged value of the thicknesses on the opposite of the center taken and it is defined as the output variables. Thus, the pre-CMP and post-CMP thicknesses are defined as follows:

$$\mathbf{y_0} = \left[y_{0,1}, y_{0,2}, \ldots, y_{0,60} \right]^T \qquad (5)$$

$$\mathbf{y} = \left[y_1, y_2, \ldots, y_{60} \right]^T \qquad (6)$$

where the subscript i (i=1-60) denotes the position on wafer from center to edge, and

$$y_i = \frac{z_{61-i} + z_{59+i}}{2} \qquad (7)$$

With the definition of the output variables and polish time, the local removal rate can be calculated by Eq. (8):

$$RR_i = \frac{\Delta y_i}{\Delta t} \qquad (8)$$

where Δy_i denotes the amount removed ($\Delta y_i = y_{0,i} - y_i$), and Δt denotes the total polish time. In modeling, the local removal rate is taken as the state variable (x) and it is also a 60x1 vector:

$$\mathbf{x} = \left[x_1, x_2, \ldots, x_{60} \right]^T \qquad (9)$$

For this multi-zone CMP, the manipulated variables are the three pressures applied:

$$\mathbf{p} = \left[p_1, p_2, p_3 \right]^T \qquad (10)$$

Note that p_{rr} is discarded here because of negligible effect on wafer surface profile. The reason is that the pressure applied to the retaining ring is to keep the wafer in an acceptable range and it has little influence on the removal rate across the radial position. After discarding p_{rr}, the experimental conditions of some sets seem to be identical. To maintain the correctness, the raw data of those sets are averaged. Therefore, there will be 14 sets of experimental data left and used in the regression.

2.3. Steady-State Analysis

From the definitions of state and input variables, the steady-state behavior for the multivariable system can be written as follows:

$$\mathbf{x} = \mathbf{K}_p \cdot \mathbf{p} \qquad (11)$$

where $\mathbf{K_p}$ is the steady-state gain matrix. Given experimental data, $\mathbf{K_p}$ matrix ($\in \Re^{60x3}$) can be determined from the least square regression. The regression result versus position on wafer is given in Fig. 2a. The effects of input pressures to the removal rate on each zone appear to be quite reasonable. The pressure applied on zone #1, p_1, shows significant effect on removal rate on the range of 0-110mm and the influence degrades gradually toward the wafer edge as can be seen from the numerical values of the first column of $\mathbf{K_p}$ (i.e., $\mathbf{K_{p1}}$). The pressure applied on the second zone, p_2, shows a large value of Preston constant around 135mm and its influence on removal rate diminishes toward both ends as shown in $\mathbf{K_{p2}}$. As expected the input pressure of the third zone shows little effect on the removal rate until 135mm and then the influence grows linearly toward to edge. However, the unusual phenomena happened on edge area, for example, the reverse trend of $\mathbf{K_{p1}}$ and the sharp decrease of $\mathbf{K_{p2}}$, are detected. Those are attributed to the effect of noise. Therefore, the final data point is excluded from now on, and a new $\mathbf{K_p}$ matrix ($\in \Re^{60x3}$) is obtained.

Let us use the singular value decomposition (SVD) to analyze the system. The SVD decomposes the $\mathbf{K_p}$ matrix of model into three matrices:

$$\mathbf{K_p} = \mathbf{U S V}^T \qquad (12)$$

where $\mathbf{U}$ is a orthonormal matrix ($\in \Re^{60x3}$) in the output side, $\mathbf{V}$ is the input orthonormal matrix ($\in \Re^{3x3}$), and $\mathbf{S}$ is a 3x3 diagonal matrix with the singular value (s_i) as the diagonal element. The ratio of the largest singular value to the smallest is the condition number ($\gamma = s_{max}/s_{min}$) which is a quantitative indicator of closeness to singularity. After proceeding SVD, the $\mathbf{V}$ matrix is found similar

to identity. Then each column of **U** matrix is plotted against position on wafer (Fig. 2b). As can be seen in the figure, the trends of the three columns in **U** matrix are quite similar to those of $\mathbf{K_p}$ matrix. It indicates that the three directions are just enough to describe the characteristic of multi-zone system. The singular values sorted by number are 264, 3 1, and 16, respectively, and condition number (?) is 16, i.e., quite far away from a singular system. Thus, this is a well-defined multivariable system with 60 states and 3 inputs.

Because of the characteristic of a non-square property of system, it is not possible to keep all 60 outputs at their set points using only 3 inputs. Thus, non-uniformity is an inherent property of this multi-zone CMP. Given the initial surface profile ($\mathbf{y}^0$) (measured) and the desired thickness $\mathbf{y}^d$, the amount needs to be removed (? $\mathbf{y}^d$) can easily calculated by

$$\Delta\mathbf{y}^d = \mathbf{y}^0 - \mathbf{y}^d \tag{13}$$

After the CMP with a polish time of ? t, the error between the desired and actual thicknesses can be expressed as

$$\begin{aligned}\mathbf{E} = \mathbf{y} - \mathbf{y}^d &= (\mathbf{y}^0 - \mathbf{y}^d) - (\mathbf{y}^0 - \mathbf{y}) \\ &= (\mathbf{x}^d - \mathbf{x}) \cdot ?\,\mathbf{t}\end{aligned} \tag{14}$$

Eq. (14) also indicates that the error is due to difference of actual removal rate ($\mathbf{x}$) and desired removal rate ($\mathbf{x}^d$). In terms of the removal rate, we have:

$$\mathbf{x}^d = \mathbf{K}_p \cdot \mathbf{p} \tag{15}$$

Solving Eq. (15) by the least-square method, the input pressures are computed:

$$\mathbf{p} = (\mathbf{K}_p^T \mathbf{K}_p)^{-1} \mathbf{K}_p^T \cdot \mathbf{x}^d = \mathbf{K}_p^\dagger \cdot \mathbf{x}^d \tag{16}$$

where the superscript † denotes the pseudo-inverse. Substituting $\mathbf{p}$ into Eq. (11), one finally obtains:

$$\begin{aligned}\mathbf{E}_{\min} &= (\mathbf{I} - \mathbf{K}_p \mathbf{K}_p^\dagger)\mathbf{x}^d \cdot ?\,\mathbf{t} \\ &= (\mathbf{I} - \mathbf{K}_p \mathbf{K}_p^\dagger) ?\,\mathbf{y}^d\end{aligned} \tag{17}$$

The above equation indicates the achievable performance for this multi-zone CMP and it is characterized by the deviation of the projection matrix ($\mathbf{K}_p \mathbf{K}_p^\dagger$) from an identity matrix. Consider the case when every entry of the vector ? $\mathbf{y}^d$ takes the value of 1. Fig. 3 shows the shape of the surface profile in the radial position. Since the 2-norm of E_{min} is equal to 0.0735, it implies an averaged error of 73.5Å for 1000Å removed.

2.4. Dynamics Analysis

After obtaining the 60x3 steady-state gain matrix, the dynamic elements which correspond to the gas holdup in each chamber are computed from the residence times. They are associated with the inputs (pressures). Assume that the flow rate of air is fixed so the time constant is proportional to the volume of the chamber in the carrier. The largest one is set to 3 s, and the others two are 0.479 s and 0.502 s, respectively. Therefore, we have a 60x3 process transfer function matrix with the same first order dynamics in each column. Moreover, from the definition of the removal rate, the removed thickness is defined as:

$$\dot{y}(t) = x(t) \tag{18}$$

Taking Laplace transformation, Eq. (18) becomes:

$$Y(s) = \frac{X(s)}{s} \tag{19}$$

where Y(s) denotes the Laplace transformed remaining thickness, X(s) is the Laplace transformed removal rate. Therefore, the polishing process can be expressed as:

$$\begin{aligned}Y(s) &= G_p(s)\,p(s) \\ &= \frac{1}{s} \cdot K_p \cdot diag\left[\frac{1}{\tau_1 s + 1}, \frac{1}{\tau_2 s + 1}, \frac{1}{\tau_3 s + 1}\right] \cdot p \\ &= \frac{1}{s} K_p D \cdot p\end{aligned} \tag{20}$$

where Gp is the process transfer function relating the input p(s) to the output Y(s), diag[.] denotes diagonal matrix, t_i stands for the time constant associated with the ith input, and D represents the diagonal matrix. Note that Gp is a 60x3 transfer function matrix with the same dynamic element in each column and the dynamics in each column is represented by a second order integrating system.

3. CONTROL

In the process control notation, the measured data are the controlled variables and the manipulated variables are the three pressures applied to each zone. Therefore, this is a 60x3 multivariable control problem. The control objective is to maintain uniform surface profile using all three manipulated variables. Because this is a non-square system, it is not possible to keep all the outputs at their set points using only 3 inputs. To the best, a least square solution, minimizing the sum of square of errors between the set point (desired thickness) and controlled variables (measured thickness), can be obtained. A 2-norm-based objective function is then considered:

$$J = \left\| \mathbf{y}^f - \mathbf{y}^d \right\|_2 \tag{21}$$

where J is the objective function, $\mathbf{y}^f$ and $\mathbf{y}^d$ are vectors ($\in \Re^{60x1}$) of measured thicknesses (at end of each run, i.e., $\mathbf{y}^f = \mathbf{y}(t_f)$) and the desired thicknesses, respectively.

Some performance indices are introduced here.

i) Standard deviation (*SD*):

$$SD = \sqrt{\sum_{i=1}^{n} (y_i^f - \overline{y}^f)^2 / n} \tag{22}$$

where the overbar stands for the mean.

ii) 8 -norm of the deviation between measured thickness and the mean:

$$\infty\text{-norm} = \left\| y^f - \overline{y}^f \right\|_\infty \tag{23}$$

iii) The range of measured thickness:

$$\text{range} = y_{\max}^f - y_{\min}^f \tag{24}$$

where $y_{\max}^f = \max(y_i^f)$ and $y_{\min}^f = \min(y_i^f)$.

iv) Non-uniformity (*NU*):

$$NU = \frac{SD}{\overline{y}^{f}} \times 100\% \quad (25)$$

Those provide simple measures of quality after polishing. Obviously, the achievable performance defined by Eq. (17) also provides an absolute basis to evaluate control performance.

3.1. Ratio Control

Since the process model, at least Kp, is perfectly know, a simple control strategy can be implemented for the multi-zone CMP process. It is a feedforward control where the ratios of the pressures are computed from the model inverse and ratios are maintained throughout the run..

The final NU in flat case is about 5% which is acceptable in the fabrication. In other cases, the first two surface profiles with small SD value, IC1 and IC2, are regarded as finer initial conditions among the three. The indices of final status of those cases are slightly more than those of achievable status. However, their NUs are both kept within 5%. The SD of final status of IC3 is reduced while the other indices are not changing much. Basically, this kind of initial surface profile is hard to handle for the system. Thus, that indicates that ECP is supported to prevent production of that profile.

3.2. Multivariable Feedback Control

It is based on concept of feedback control. The controller adjusts the pressure input simultaneously according to the deviation between measured thickness by sensor and set points (desired thickness). To monitor the change of surface in a polish run, therefore, an *in situ* sensor is required to measure copper thickness on-line and a non-square feedback controller necessary to generate input pressures. Fig. 4a shows the non-square system with the tall process (more output than inputs) and a fat controller (more input to the controller than the control output). The SVD-based approach is employed to design the inversed-based controller. First, the steady-state gain matrix is decomposed into three matrices and the multivariable system can be expressed as (Fig. 4b):

$$\mathbf{Y} = \frac{1}{s}\mathbf{K}_{\mathbf{p}} \cdot \mathbf{D} \cdot \mathbf{p} = \frac{1}{s}(\mathbf{U}\Sigma\mathbf{V}^{T})\mathbf{D} \cdot \mathbf{p} = \mathbf{U} \cdot diag[\frac{\sigma_i}{s}] \cdot \mathbf{V}^{T} \cdot \mathbf{D} \cdot \mathbf{p} \quad (26)$$

Next, the derivative part of the controller is taken as the inverse of **D** and the output of the PI part of the controller becomes:

$$\mathbf{p} = \mathbf{D}^{-1}\mathbf{p}_{PI} \quad (27)$$

Thus, the relationship between the p_{PI} and Y becomes:

$$\mathbf{Y} = \mathbf{U} \cdot diag[\frac{\sigma_i}{s}] \cdot \mathbf{V}^{T}\mathbf{p}_{PI} \quad (28)$$

Multiply the both sides with $\mathbf{U}^{\mathbf{T}}$ matrix (recall that both **U** and **V** are orthonormal matrices, i.e., $\mathbf{U}\mathbf{U}^{T} = I$ and $\mathbf{V}^{T}\mathbf{V} = I$), one obtains:

$$\mathbf{U}^{T}\mathbf{Y} = diag[\frac{\sigma_i}{s}] \cdot \mathbf{V}^{T} \cdot \mathbf{p}_{PI} \quad (29)$$

$\mathbf{U^{T}Y}$ and $\mathbf{V^{T}p_{PI}}$ correspond to the output and input in the principle directions and they are defined as $\mathbf{Y}^{*}$ ($\in \Re^{3x1}$) and $\mathbf{p}^{*}$($\in \Re^{3x1}$), respectively. Therefore, we are left with a decoupled square system with simple diagonal elements, σ_i / s . Define the diagonal matrix as $\mathbf{G_p}^{*}$, the multivariable system becomes:

$$\mathbf{Y}^{*} = G_p^{*}\mathbf{p}^{*} \quad (30)$$

Fig. 4c also shows the result of transformation. Note the diagonalizing effort is absorbed into the controller as shown in Fig. 4b. Therefore, standard multivariable control method can be applied to this decoupled square system.

The internal model control (IMC) principle is employed to design the PID type of multivariable controller. In the IMC design, the relationship between the IMC controller (C_{IMC}) and the diagonal PI controller (C_{PI}) is:

$$C_{IMC} = [I + C_{PI}\hat{G}_p^{*}]^{-1}C_{PI} \quad (31)$$

where $\hat{G}_p^{*}$ is the model of the process. The IMC design consists of the following steps:

i. Decompose the diagonal process model $\hat{G}_p^{*}$ into:

$$\hat{G}_p^{*}(s) = \hat{G}_p^{+}(s) \cdot \hat{G}_p^{-}(s) \quad (32)$$

where $\hat{G}_p^{+}$ represents the terms of time delay and all the right-half plane zeros, $\hat{G}_p^{-}$ represents the invertible part. Since the system doesn't contain any non-minimum phase element, $\hat{G}_p^{*}(s)$ is equal to $\hat{G}_p^{-}(s)$.

ii. Because the trajectory for the removed thickness is a ramp function (increase linearly with time), the type-2 input is assumed for the design of the controller. Thus, the IMC filter (**F**) is chosen as:

$$\mathbf{F} = diag[f_i] \quad (33)$$

, and

$$f_i = \frac{2\tau_{CL,i}s + 1}{(\tau_{CL,i}s + 1)^{2}} \quad (34)$$

where $t_{CL,i}$ is the closed-loop (filter) time constant in each loop. In this work, the filter time constant is set to 30% of the open-loop time constant.

iii. The IMC controller is thus obtained.

$$C_{IMC} = (\hat{G}_p^{*})^{-1}\mathbf{F} \quad (35)$$

Substituting C_{IMC} into Eq. (34), and the diagonal PI controller (C_{PI}) becomes:

$$C_{PI} = C_{IMC}[I - \hat{G}_p^{*}C_{IMC}]^{-1} = (\hat{G}_p^{-}(s))^{-1}\frac{f_i}{1 - f_i} \quad (36)$$

In a matrix form, the diagonal multivariable PI controller becomes:

$$C_{PI} = \Sigma^{-1} \cdot \begin{bmatrix} \frac{2\tau_{CL,1}s+1}{\tau_{CL,1}^2 s} & 0 & 0 \\ 0 & \frac{2\tau_{CL,2}s+1}{\tau_{CL,2}^2 s} & 0 \\ 0 & 0 & \frac{2\tau_{CL,3}s+1}{\tau_{CL,3}^2 s} \end{bmatrix} \quad (37)$$

Once the diagonal controllers become available, the full multivariable PID controller can be obtained by pre-multiplying the inverse of dynamic element ($\mathbf{D}^{-1}$) and the $\mathbf{V_c}$ matrix (from the SVD) (Fig. 4b). The resultant controller C_{PID} becomes:

$$C_{PID} = \begin{bmatrix} v_{11}C_{PI,1}(\tau_1 s+1) & v_{12}C_{PI,2}(\tau_1 s+1) & v_{13}C_{PI,3}(\tau_1 s+1) \\ v_{21}C_{PI,1}(\tau_2 s+1) & v_{22}C_{PI,2}(\tau_2 s+1) & v_{23}C_{PI,3}(\tau_2 s+1) \\ v_{31}C_{PI,1}(\tau_3 s+1) & v_{32}C_{PI,2}(\tau_3 s+1) & v_{33}C_{PI,3}(\tau_3 s+1) \end{bmatrix} \quad (38)$$

This multivariable controller consists of a diagonal PI type of controller, a $\mathbf{V_c}$ matrix which is generated from the SVD of system, and an inverse matrix of $\mathbf{D}$ (containing the derivative term). Thus, it becomes a full multivariable PID controller. Each element of this multivariable controller can be expressed analytically:

$$c_{PIDij} = \sigma_i^{-1} v_{ij} \cdot \left(\left(\frac{\tau_i + 2\tau_{CL,i}}{\tau_{CL,i}^2}\right) + \left(\frac{1}{\tau_{CL,i}}\right)\frac{1}{s} + \left(\frac{2\tau_i}{\tau_{CL,i}}\right)s \right) \quad (39)$$

In terms of PID settings, the controller parameters, proportional gain, reset time and derivative time, thus become:

$$K_{cij} = \frac{v_{ij}(\tau_i + 2\tau_{CL,i})}{\sigma_i \tau_{CL,i}^2} \quad (40)$$

$$\tau_{Iij} = \frac{v_{ij}}{\sigma_i \tau_{CL,i}} \quad (41)$$

$$\tau_{Dij} = \frac{2v_{ij}\tau_i}{\sigma_i \tau_{CL,i}} \quad (42)$$

Taking the flat profile as an example, Fig. 5a shows the snapshots of the surface profiles throughout the polishing process. The control performance can be seen from the responses of the manipulated variables (Fig. 5 b & c) and the tracking error (Fig. 5d). In terms of the principle output (Fig. 5d) and input (Fig. 5c), the output settles to the set point in less than 20 seconds and acceptable control performance is obtained using the SVD-based multivariable controller. For CMP process, the ultimate performance measure in the uniformity. Table 1 summarizes all the indices using the ratio control as well as the multivariable feedback control. Comparison is made with respect to the achievable performance (Table 1). Results clearly indicate that the multivariable feedback control leads to the performance close to the achievable performance while the ratio control shows 4-15% deviations from the achievable one. More importantly, the seemingly complex control system can be design systematic manner with rather standard feedback design methodology.

4. CONCLUSION

In this work, a systematic modeling and control system design approaches are proposed for a multi-zone CMP system. The multi-zone CMP is intended to reduce the within-wafer non-uniformity (WIWNU) by manipulating different pressures across the radial position. This leads to a non-square multivariable system, a 60x3 system for the example studied. In the modeling phase, two 2^3 full factorial experimental design is carried out and steady-state gain matrix is obtained from the lease square regression followed by including the dynamic element associated with each input. For multivariable control, two control strategies with different degrees of complexity are proposed. First, a simple ratio control is designed based on the pseudo-inverse of the process model and, provided with the initial surface profile, the input pressures are computed and the ratios are maintained throughout the polishing run. The results show that, while giving reasonable uniformity, the performance is a little short from the achievable performance. Next, an on-line multivariable control system is designed. The singular value decomposition (SVD) is used to project the input and output in the principle directions and, therefore, the controllers can be designed in a reduced dimension (3x3) for a decoupled system. Then, the diagonal controllers are transformed back to the true input/output spaces. This significantly reduces the engineering effort in control system design. Results show that achievable control performance can be maintained using the SVD-based multivariable controllers.

ACKNOWLEDGEMENT

SJS and CCY thank National Science Council of Taiwan for the financial support under the grant NSC 92-2214-E002-032.

REFERENCES

Edgar, T. F.; S. W. Butler; W. J. Campbell; C. Pfeiffer; C. Bode; S. B. Hwang; K. S. Balakrishnan; J. Hahn, *"Automatic control of microelectronics manufacturing: practices, challenges and possibilities", Automatica, **36**, 1567-1603 (2000).*

Kao, Y. C.; C. C. Yu; S. H. Shen *"Robust Operation of Copper Chemical Mechanical Polishing", Microelectronic Eng., **65**, 61-75 (2002).*

Preston, F. W., "The theory and design of plate glass polishing machines", *J. Soc. Glass Technology*, 11, 214-256 (1927).

Yao, C. H.; D. L. Feke; K. M. Robinson; S. Meikleb, "The influence of feature-scale surface geometry on CMP processes", *J. Electrochem. Soc.*, **147**, 3094-3099 (2000).

Table 1. Different uniformity measures of wafer surfaces before and after CMP using ratio control, multivariable feedback control and achievable performance (from Eq. 17) also given for comparison

Surface profile		Flat	IC1	IC2	IC3
Initial	SD	0	62.21	88.47	159.4
	8-norm	0	378	636	603
	range	0	444	714	734
	NU (%)	0	0.71	1	1.15
Achievable	$\|E_{min}\|_2$	727	535	698	1170
	SD	95.46	70.3	91.61	153.6
	8-norm	189	142	321	457
	range	363	272	541	802
	NU (%)	4.77	3.51	4.58	7.68
Final (Top: ratio control Bottom: *multivariable feedback control*)	$\|E\|_2$	786 *751*	618 *579*	740 *703*	1218 *1201*
	SD	101 *95.23*	77.5 *70.04*	97 *91.52*	157 *153.33*
	8-norm	225 *189*	223 *143*	330 *322*	444 *455*
	range	379 *362*	345 *273*	528 *541*	778 *800*
	NU (%)	5.01 *4.7*	3.83 *3.45*	4.83 *4.55*	7.72 *7.53*
Relative error*		8.12 *3.3*	15.51 *8.22*	6.02 *0.72*	4.1 *2.65*

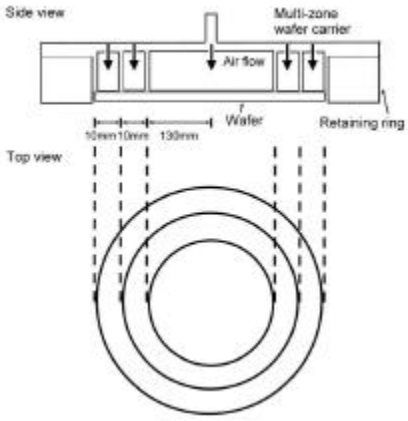

Fig. 1. Configuration of multi-zone CMP.

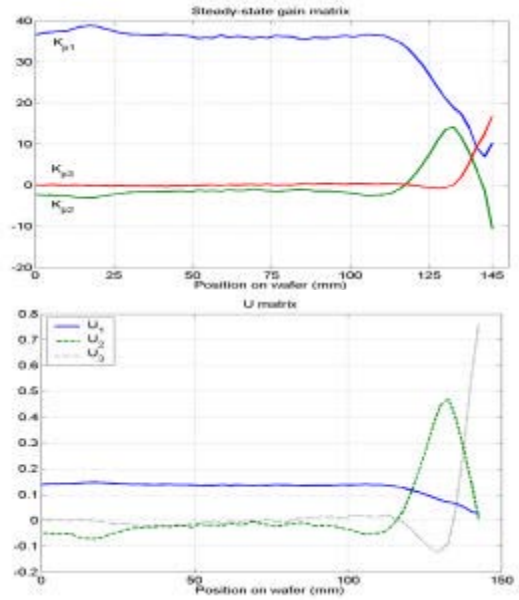

Fig. 2. Steady-state gain vectors and vectors of the U matrix from SVD

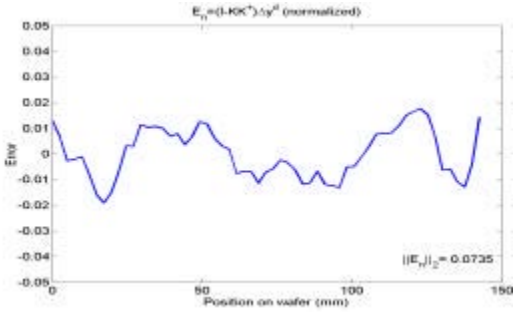

Fig. 3. The error vector of achievable performance by assuming input vector of unity.

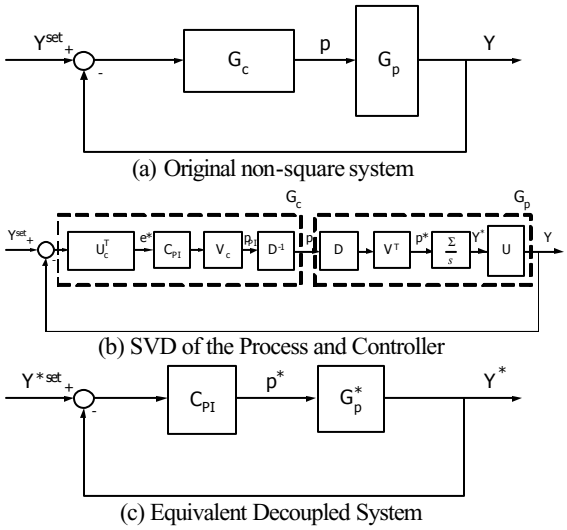

Fig. 4. Evolution of the SVD-based design and corresponding block diagrams.

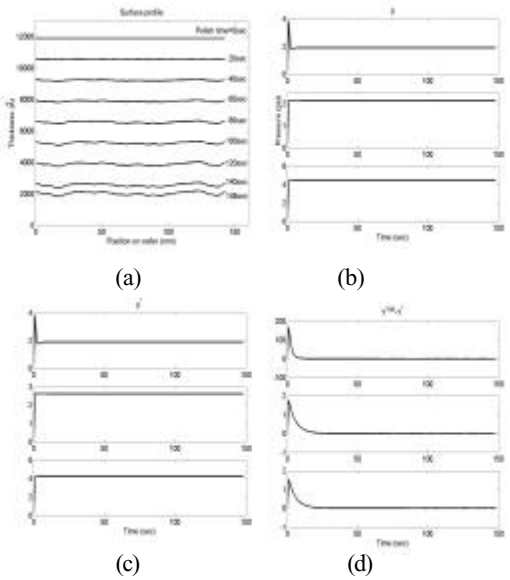

Fig. 5. Results of multivariable feedback control for incoming wafer with flat profile: (a) snap shots of surface profile, (b) pressures, (c) principal input, and (d) error in the principle direction.